SUPPLEMENT

Supplemental Data

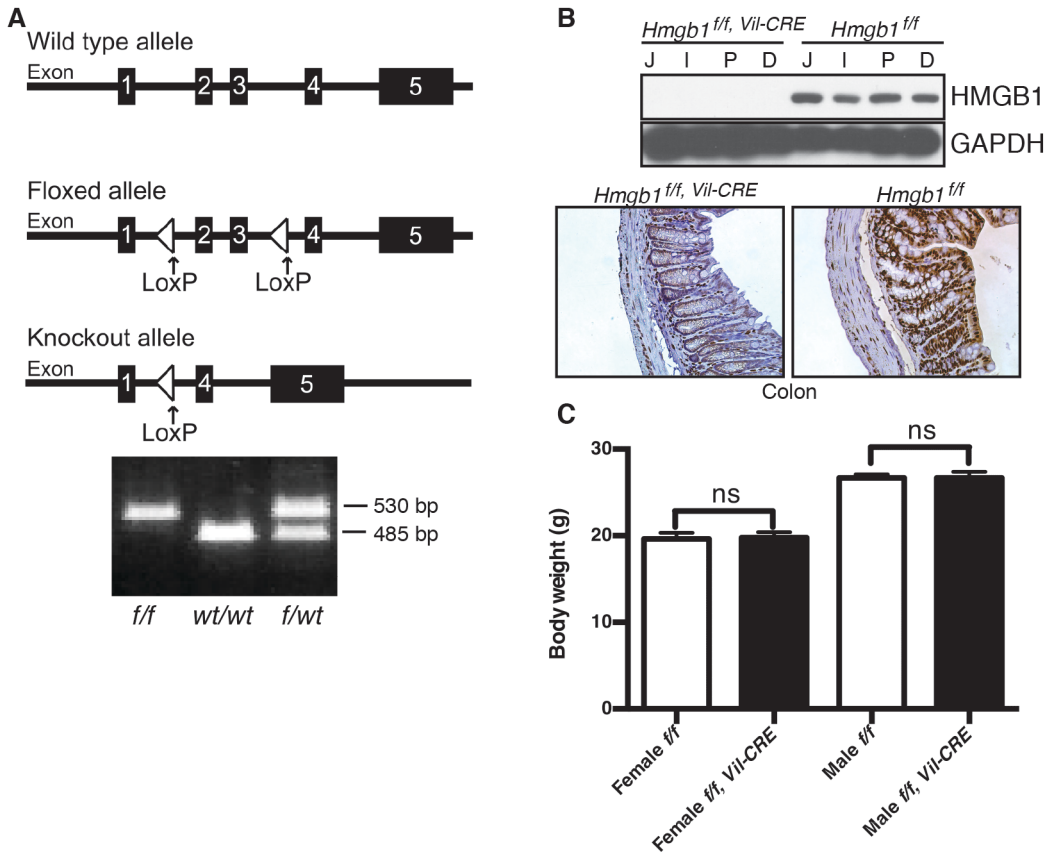

Supplementary Figure 1: Generation and characterization of *Hmgb1*$^{f/f,\ Vil\text{-}CRE}$ mice.
A, *Hmgb1*$^{f/f}$ mice were generated by flanking exons 2 and 3 of the gene with LoxP sites. Breeding *Hmgb1*$^{f/f}$ mice to mice expressing CRE-recombinase under the villin promotor resulted in deletion of the *Hmgb1* start codon and a frame shift resulting in early termination of translation in intestinal epithelial cells. Genotyping PCR produced a 485 bp band from wild type alleles (WT) and a 530 bp band from floxed alleles (F). **B,** HMGB1 expression in the jejunum (J), ileum (I), proximal colon (P), and distal colon (D) of *Hmgb1*$^{f/f}$ (n= 3) and *Hmgb1*$^{f/f,\ Vil\text{-}CRE}$ (n=3) mice evaluated by immunoblotting. Intestinal sections from untreated *Hmgb1*$^{f/f}$ and *Hmgb1*$^{f/f,\ Vil\text{-}CRE}$ mice stained with hematoxylin, eosin, and anti-HMGB1 antibody (200X magnification). **C,** Weight of age and sex-matched *Hmgb1*$^{f/f}$ (n= 8 female and n=11 male) and *Hmgb1*$^{f/f,\ Vil\text{-}CRE}$ (n=11 female and n=7 male) mice. (mean ± s.e.m) Data analyzed using two-tail T-tests.

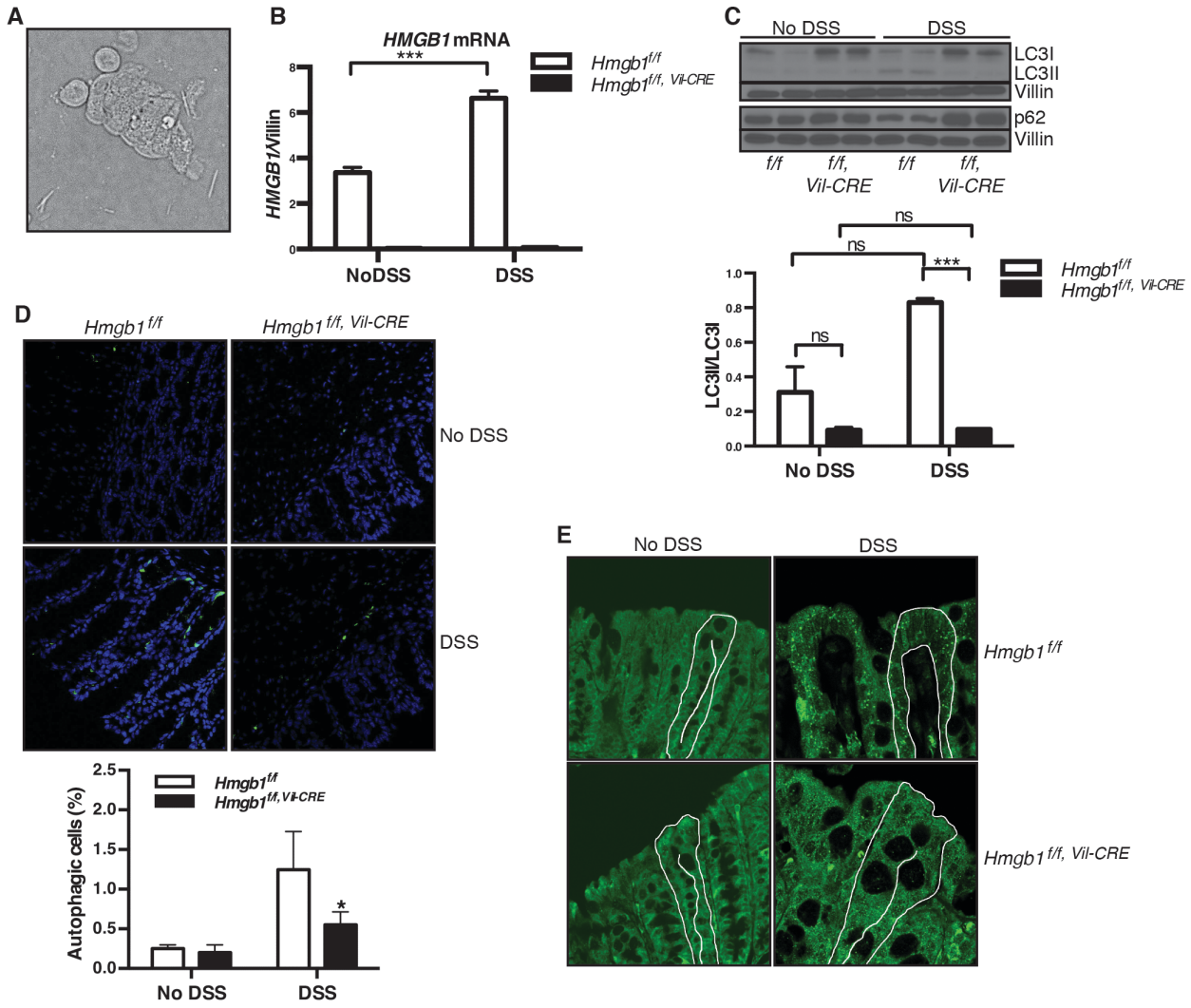

Supplementary Figure 2: HMGB1 loss compromises autophagy in IEC.

A, Phase-contrast microscopy of EDTA isolated IEC (100X magnification). **B,** Quantitative real-time PCR for HMGB1 expression in EDTA-isolated IEC. (mean ± s.e.m.) **C,** Immunoblotting for LC3B and p62 in EDTA-isolated IEC cells from *Hmgb1*$^{f/f}$ (n=4) and *Hmgb1*$^{f/f, Vil\text{-}CRE}$ (n=4) mice. The LC3II/LC3I ratio is reported as the mean ± s.e.m. **D,** Confocal microscopy of GFP-LC3 in colon sections obtained from *Hmgb1*$^{f/f}$ (n=5) and *Hmgb1*$^{f/f, Vil\text{-}CRE}$ (n=5) mice crossed to GFP-LC3 reporter mice (200X magnification). **E**, Images from **Figure 2E** with outlines showing the position of IEC in the intestine (630X magnification). These cells are arranged along the luminal side of the intestinal mucosa. Black circles devoid of staining are mucus droplets within IEC. Data analyzed using two-tail T-tests. *P<0.05; **P<0.01; ***P<0.005, ****P<0.001

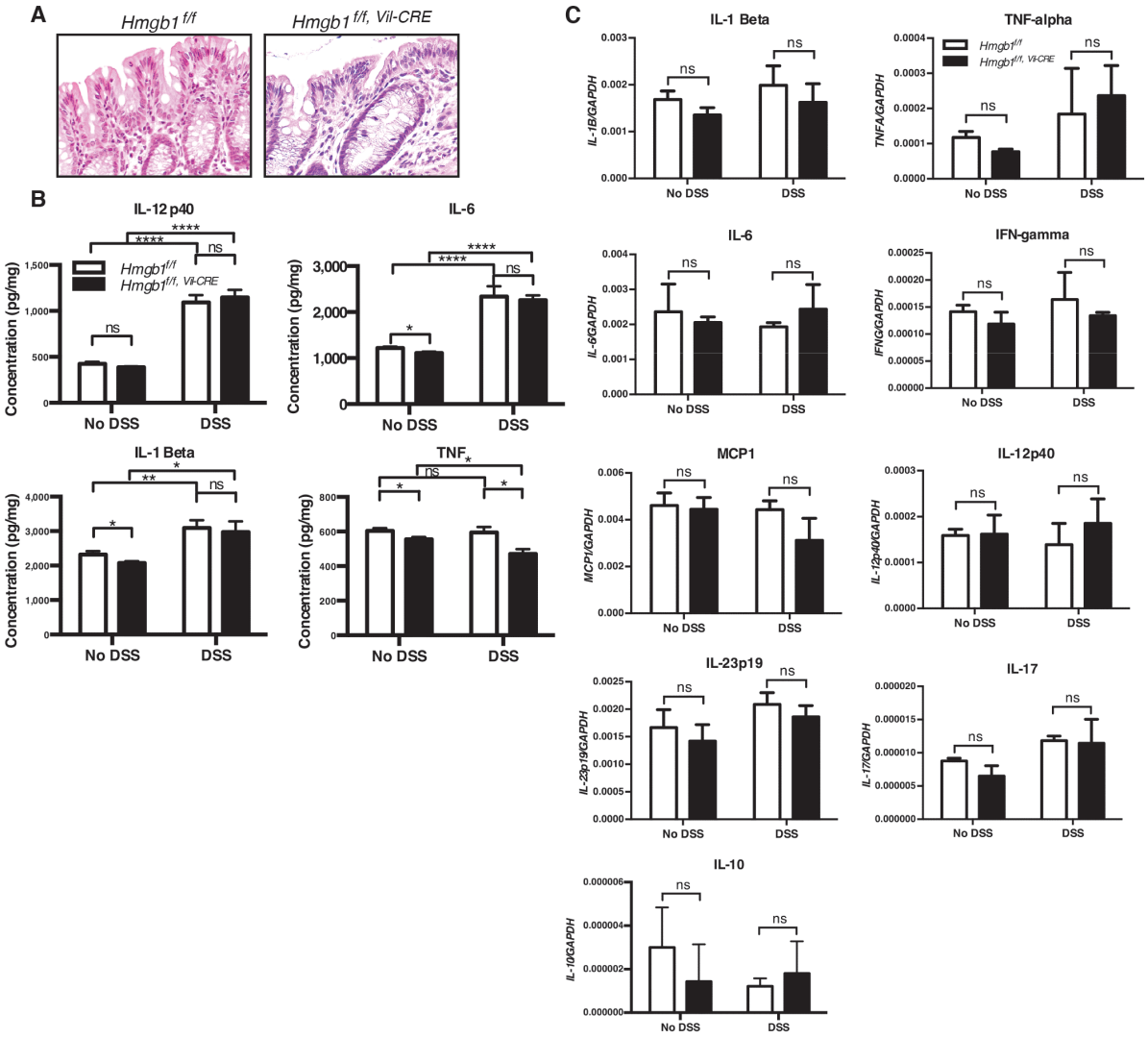

Supplemental Figure 3: Intestinal epithelial cell death preceeds adaptive immune system activation in *Hmgb1*$^{f/f,\ Vil\text{-}CRE}$ mice treated with DSS.

A, Hematoxylin and eosin staining of formalin-fixed and paraffin-embedded colon from *Hmgb1*$^{f/f}$ (n=4) and *Hmgb1*$^{f/f\text{-}Vil\text{-}CRE}$ (n=4) mice treated with 3 days of DSS (200X magnification). **B,** Cytokine protein expression in the colonic mucosa on day 3 of DSS from *Hmgb1*$^{f/f}$ (n=8) and *Hmgb1*$^{f/f\text{-}Vil\text{-}CRE}$ (n=8) mice. (mean ± s.e.m.) **C,** Cytokine mRNA expression in the colonic mucosa of DSS-treated (day 3) *Hmgb1*$^{f/f}$ (n=3) and *Hmgb1*$^{f/f\text{-}Vil\text{-}CRE}$ (n=3) mice. (mean ± s.e.m.) Data analyzed using two-tail T-tests. *P<0.05; **P<0.01; ***P<0.005, ****P<0.001

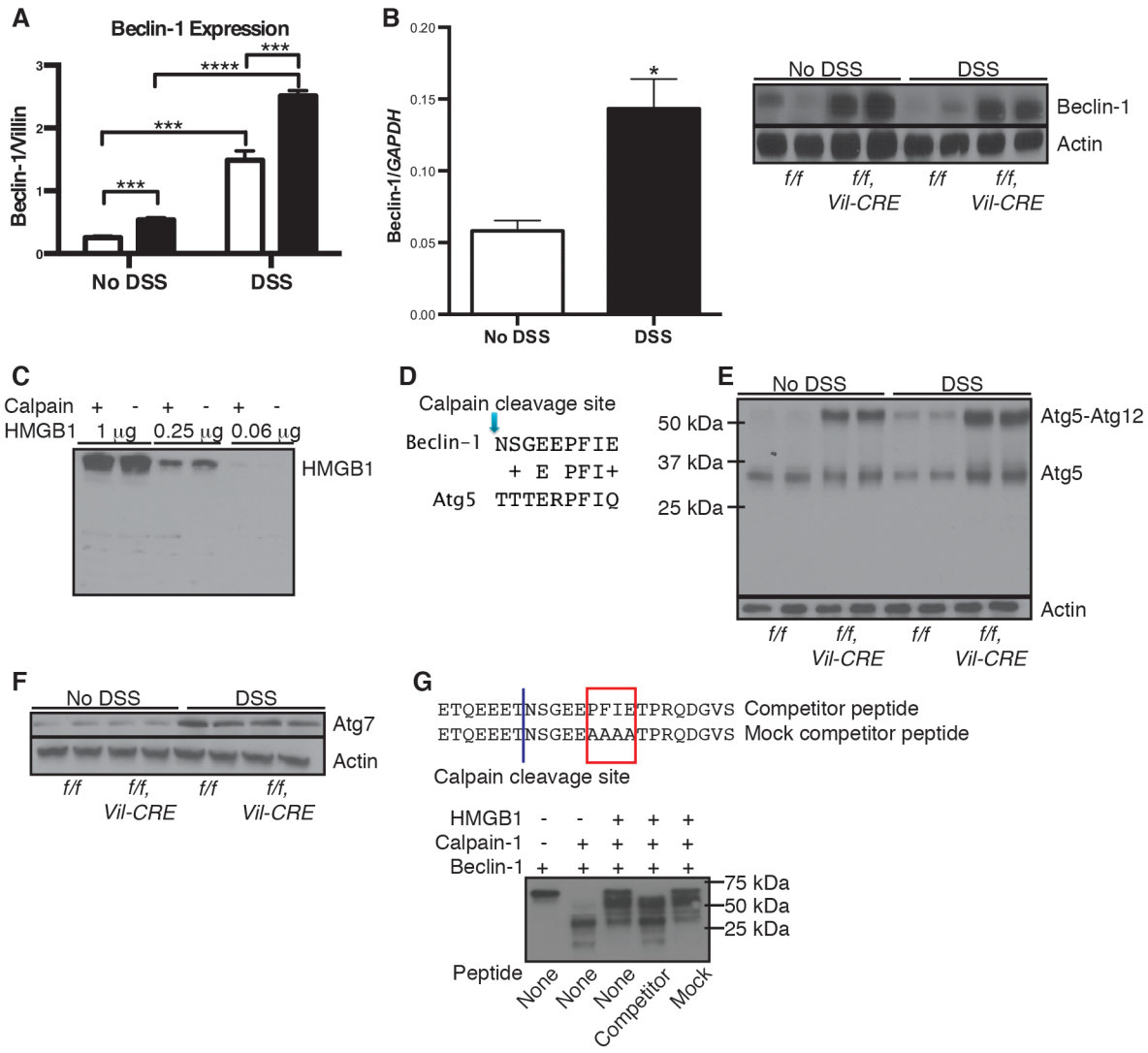

Supplementary Figure 4: HMGB1-mediated protection from calpain cleavage.
A, Quantitative RT-PCR for beclin-1 performed on EDTA-isolated IEC samples. (mean ± s.e.m.) **B,** Quantitative RT-PCR (*Hmgb1*$^{f/f}$ n=6 and *Hmgb1*$^{f/f,\ Vil\text{-}CRE}$ n=6) and immunoblotting (*Hmgb1*$^{f/f}$ n=4 and *Hmgb1*$^{f/f,\ Vil\text{-}CRE}$ n=4) for beclin-1 in mucosal scrapings from mice on day 3 of DSS. (mean ± s.e.m.) Beclin-1 antibody was raised against an epitope surrounding amino acid 72 of the protein. This antibody does not recognize cleaved beclin-1. **C,** Immunoblotting of the products from a calpain cleavage assay containing the indicated amounts of HMGB1 and 0.5 units of active calpain. **D,** Sequence alignment of beclin-1 and Atg5 in the area of the calpain-cleavage site. **E,** Immunoblotting for Atg5 with antibody raised against residues in the carboxy terminus of the protein. This antibody does not recognize cleaved Atg5. **F,** Immunoblotting for Atg7 in mucosal scrapings from *Hmgb1*$^{f/f}$ (n=4) and *Hmgb1*$^{f/f,\ Vil\text{-}CRE}$ (n=4) mice treated with DSS for 3 days. **G**, Beclin-1 immunoblot of the products from an in vitro HMGB1 protection assay. Beclin-1 was incubated with active calpain-1, HMGB1, and a competitor or mock competitor peptide. Data analyzed using two-tail T-tests. *P<0.05; **P<0.01; ***P<0.005, ****P<0.001

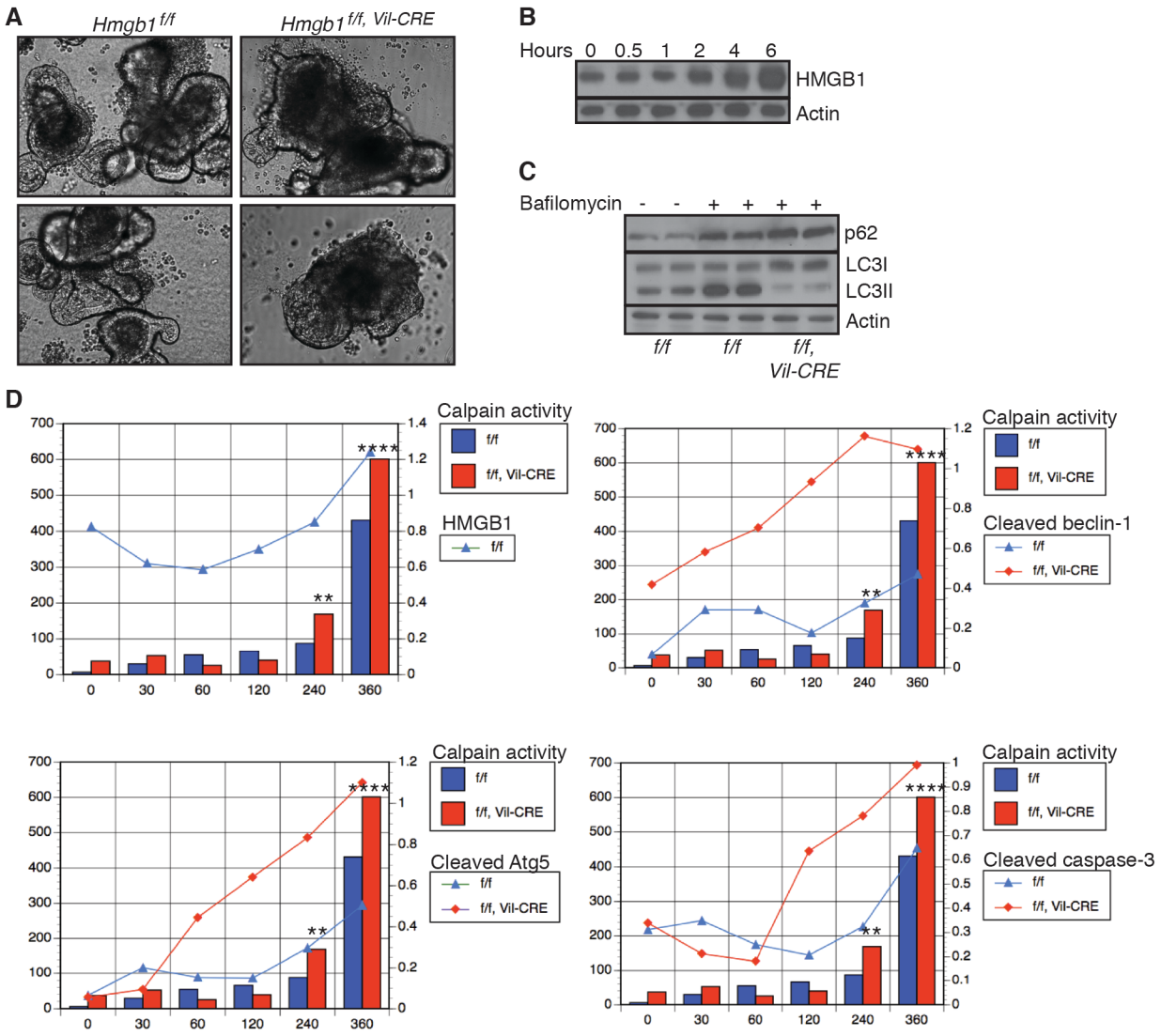

Supplementary Figure 5: HMGB1 expression and calpain activity in cultured enteroids. **A,** Phase constrast microscopy of intestinal enteroids in culture (200X magnification). **B,** Immunoblotting for HMGB1 expression over time in enteroids treated with 10 µg/ml L-18 MDP. **C,** Immunoblotting for LC3B and p62 in lysates from enteroids treated with 10 µg/ml L-18 MDP in the presence or absence of 100 nM bafilomycin A1 for four hours. **D,** Graphical representation of cleavage of beclin-1, Atg5, and caspase-3 and HMGB1 expression over time versus mean calpain activity. In each of the graphs, the calpain activity is represented on the left axis in RFU/mg/min, the protein is represented on the right axis as protein/actin, and the x axis is the time in minutes. Asterisks pertain to the calpain activity. Graphs generated using data from **Figure 5F, G, H, I** and (**B**). *P<0.05; **P<0.01; ***P<0.005, ****P<0.001

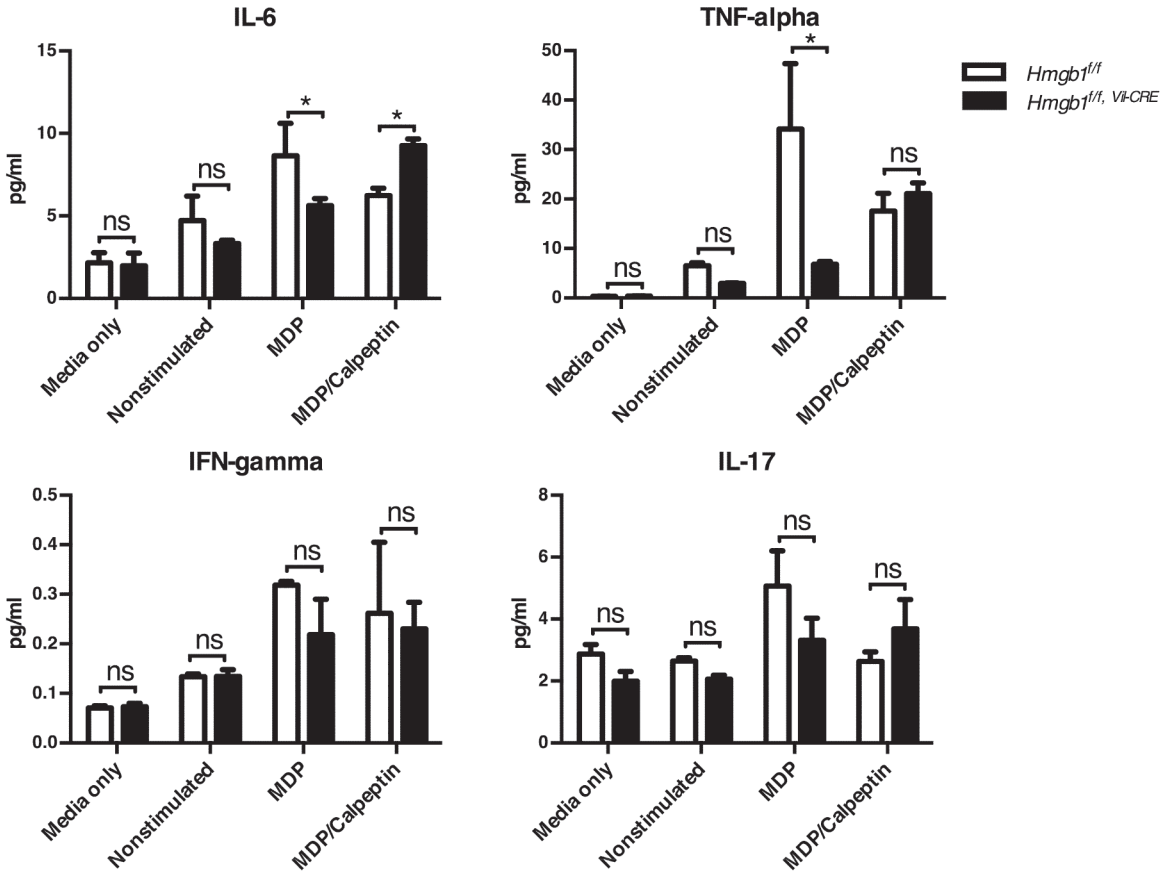

Supplemental Figure 6: Loss of HMGB1 does not increase the pro-inflammatory nature of IEC death in response to MDP.

Cytokine expression measured by ELISA from mesenteric lymph node cultures stimulated with supernatants of enteroids (*Hmgb1*$^{f/f}$ n=4 and *Hmgb1*$^{f/f,\ Vil\text{-}CRE}$ n=4) treated with 10 µg/ml L-18 MDP for four hours in the presence of vehicle (DMSO) or 1 µg/ml calpeptin. (mean ± s.e.m.) Data analyzed using two-tail T-tests. *P<0.05; **P<0.01; ***P<0.005, ****P<0.001

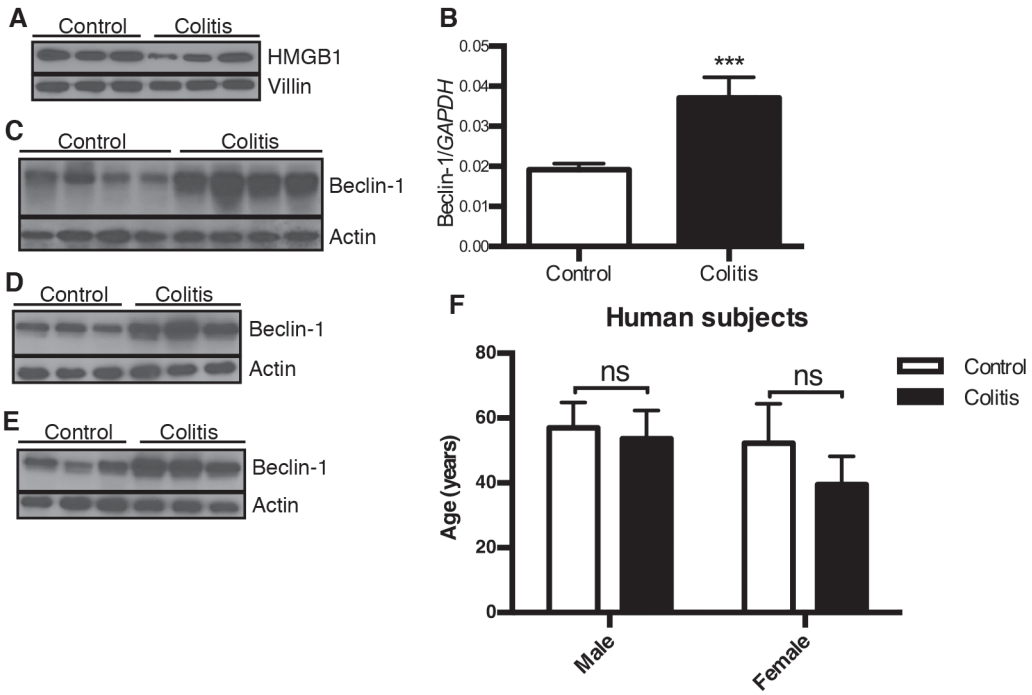

Supplementary Figure 7: Additional data from human subjects.
A, Immunoblotting for HMGB1 in lysates of intestinal epithelial biopsies. Lane (1) Control/normal, (2) Control/normal, (3) Control/quiescent Crohn's disease (CD), (4) UC/moderate, (5) UC/moderate, and (6) CD/severe. **B**, Quantitative PCR for beclin-1 expression (mean ± s.e.m.) **C,** Immunoblotting for beclin-1 in lysates of intestinal epithelial biopsies. Lanes (1) to (4) controlled Crohn's disease and lanes (5) to (8) active Crohn's disease patients. **D,** Immunoblotting for beclin-1 in lysates of intestinal epithelial biopsies. Lanes (1) to (3) normal controls (4) to (6) active ulcerative colitis patients. **E,** Immunoblotting for beclin-1 in lysates of intestinal epithelial biopsies. Lanes (1) to (3) normal controls (4) to (6) active Crohn's disease patients. **F**, Age and sex of humans whose biopsies were analyzed in these studies. (mean ± s.e.m.) Data analyzed using two-tail T-tests. *P<0.05; **P<0.01; ***P<0.005, ****P<0.001